Impact of phosphorescent dye on the performance and impedance spectroscopy for P3HT:PCBM solar cells

Amr Attia Abuelwafa[1,2] · Sahar Elnobi[1] · R. MD Matiur[2] · M. Dongol[1] · M. M. El-Nahass[3] · T. Soga[2]

Abstract

In this research, we examined the influence of platinum octaethylporphyrin (PtOEP) concentration on the photovoltaic and impedance spectroscopy of P3HT:PCBM solar cells. Through optimizing the concentration of PtOEP in the blend, the average power conversion efficiency of P3HT:PCBM solar cells was raised from 3.06 to 3.61%, when milligram of PtOEP was added to the blend. According to the impedance spectroscopy, the low concentration of PtOEP significantly increases the recombination process, simultaneously increasing the diffusion coefficient (D) and charge-carrier mobility (μ). These findings suggest that the incorporation of low doses of PtOEP into P3HT:PCBM blends will be a practical method for achieving the high efficiency of polymer solar cells.

Graphical abstract
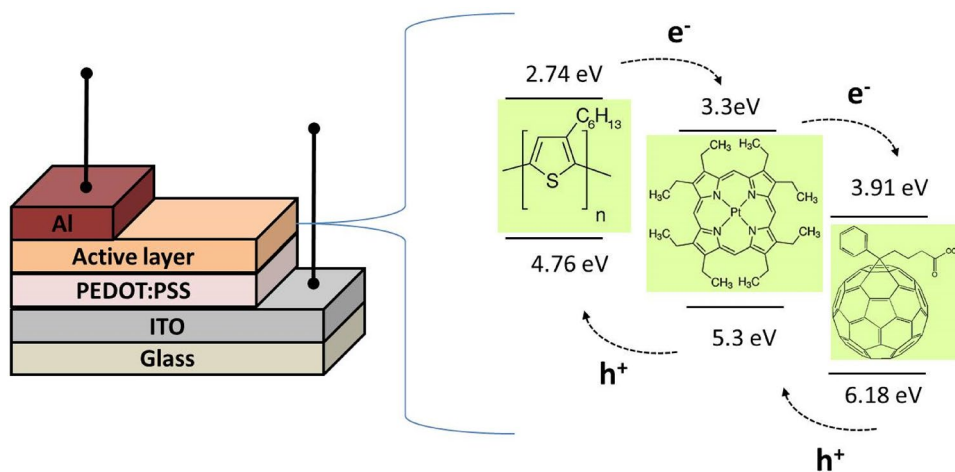
1 Introduction

Due to their lightweight, low cost, simplicity of large-scale production, and compatibility with flexible substrates, polymer solar cells (PSCs) are the most potent renewable energy source [1]. Numerous attempts have been made recently to improve the performance and reliability of PSCs, including the use of novel materials for greater photon collecting, interface modification for improved charge-carrier

✉ Amr Attia Abuelwafa
   Amr.abuelwafa@sci.svu.edu.eg

1   Nano and Thin Film Lab, Physics Department, Faculty
    of Science, South Valley University, Qena 83523, Egypt

2   Department of Electrical and Mechanical Engineering,
    Nagoya Institute of Technology, Nagoya 466-8555, Japan

3   Physics Department, Faculty of Education, Ain Shams
    University, Roxy 11757, Cairo, Egypt

Fig. 1 Schematic view of the ITO/PEDOT:PSS/ P3HT:PCBM:PtOEP/Al solar cell architecture and the chemical structure of P3HT:PCBM:PtOEP with the energy levels
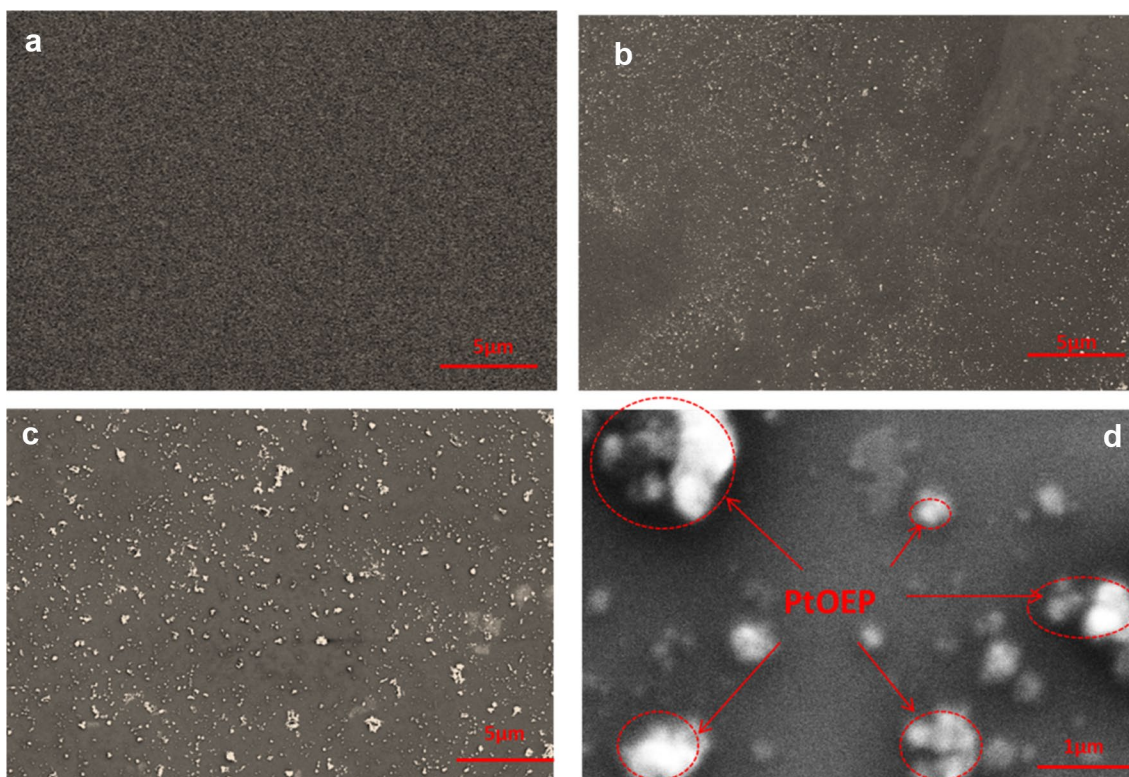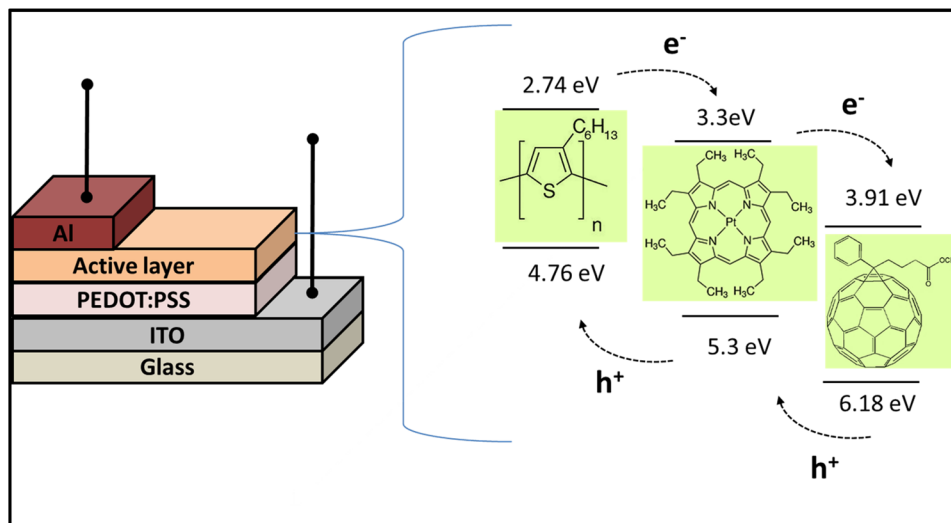

Fig. 2 SEM image of P3HT:PCBM **a** without doping, **b** 2 mg mL^{-1} doping, **c** 6 mg mL^{-1} doping, and **d** 6 mg mL^{-1} doping at higher magnification

selection, and the deployment of novel designs [1–4]. In addition, a range of procedures, including heat annealing, solvent vapor annealing, and doping processes, have been successfully employed to improve the carrier's electrical conductivity, shape, and solar cell capacity [4–8]. Following light absorption, photocurrent production occurs in multiple phases, including the creation of excitons, their diffusion to the donor (D)/acceptor (A) interface, their free dissociation, and their transport to the electrodes. Numerous variables contribute to inefficiency. One is recombination at the D/A
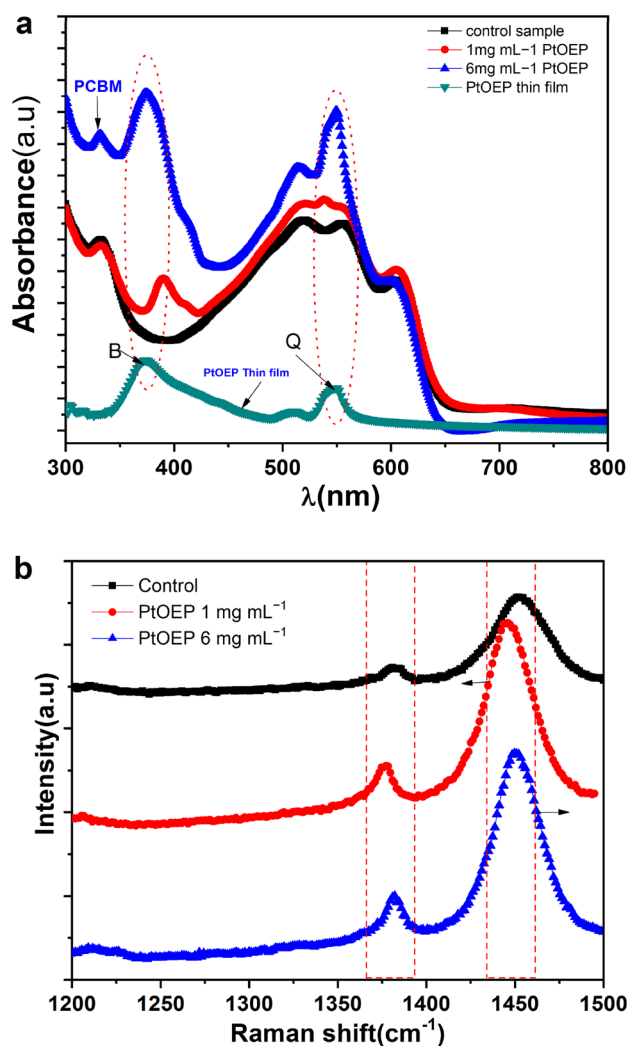
Fig. 3 **a** Absorption spectra of PtOEP thin film, P3HT:PCBM (1, 6 mg mL^{-1}) and **b** Raman spectra for P3HT:PCBM:PtOEP (0, 1, 6 mg mL^{-1})

contact, which prevents excitons from diffusing. As a result, we need to find a strategy to improve the diffusion length in order to optimize the performance of solar cells. It is widely established that phosphorescent dyes or triplet-exciton materials have a greater diffusion length and lifespan. Increase the photocurrent effectively by converting singlet excitons to triplet excitons [9–13]. If singlet excitons can be changed by intersystem crossing into triplet excitons with a longer lifespan, this would benefit exciton dissociation. Using strong atomic effects to boost the performance of polymer solar cells by doping phosphorescent elements such as PtOEP into organic solar cells is a feasible technique. The purpose of this study is to explore the influence of various concentrations of PtOEP, a phosphorescent dye, on the efficiency and impedance spectroscopy (IS) of P3HT:PCBM PSCs.

2 Experimental

2.1 Film and solar cells' fabrication

PtOEP (Sigma-Aldrich) was added amounts 0.5, 1, 2, 3, and 6 mg per 20 mg mL^{-1} of P3HT[Mw 50,000–100,000]:PCBM[Mw 910.88] (1:1) (Sigma-Aldrich) and then combined with 1, 2-dichlorobenzene as a solvent. The blends were dynamically stirred at160 rpm under 60 °C for 24 h. To fabricate the solar cell, a layer of poly(3,4-ethylenedioxythiophene)-blend-poly(styrene-sulfonate) (PEDOT:PSS) (Sigma-Aldrich) was spin-coated (at 4000 rpm for 30 s) on top of clean ITO(10/square) substrates in the air and was dried by thermal annealing using a digitally controlled hotplate at 150 °C for10 min. The P3HT:PCBM:PtOEP blends solution was spin-coated at 1500 rpm for 30 s on the top of insoluble PEDOT:PSS layer with annealing for eliminating any remaining solvent at 150 °C for 5 min under nitrogen N$_2$ atmosphere in a glove box. The Al electrode (~100 nm) was thermally deposited onto the active layer using a vacuum deposition system at a pressure of about 2×10^{-4} Pa through a shadow mask to obtain 20 identical cells on one device with an active area of 0.09 cm^2. The complete organic solar cells [ITO/PEDOT:PSS/P3HT:PCBM:PtOEP/Al], with a configuration, are displayed in Fig. 1.

2.2 Measurements

Scanning electron microscopy (SEM, JEOL model JSM-6510) was used to investigate the morphology of the samples at room temperature, and the Raman spectrum was determined using a Raman Spectrometer (Jasco NRS-2100). A spectrophotometer was used to record the optical absorption spectra (JASCO V-570). The external quantum efficiency (EQE) measurements were performed with a halogen lamp and a monochromatic filter. The J/V parameters of the cells were determined using a computer-controlled voltage-current source meter under standard solar irradiation of 100 mW/cm^2 (AM1.5 G) at 25 °C (Keithley 238). The IS in the dark was determined at room temperature in the air using an impedance analyzer (Agilent 4284A) at a bias voltage of.

3 Results and discussion

Figure 2a illustrates the effect of PtOEP doping on P3HT:PCBM absorption. In the absorption spectra of the blends, the bands of PtOEP [14, 15] are observed at 374 and 547 nm, respectively. In addition, it is obvious that the
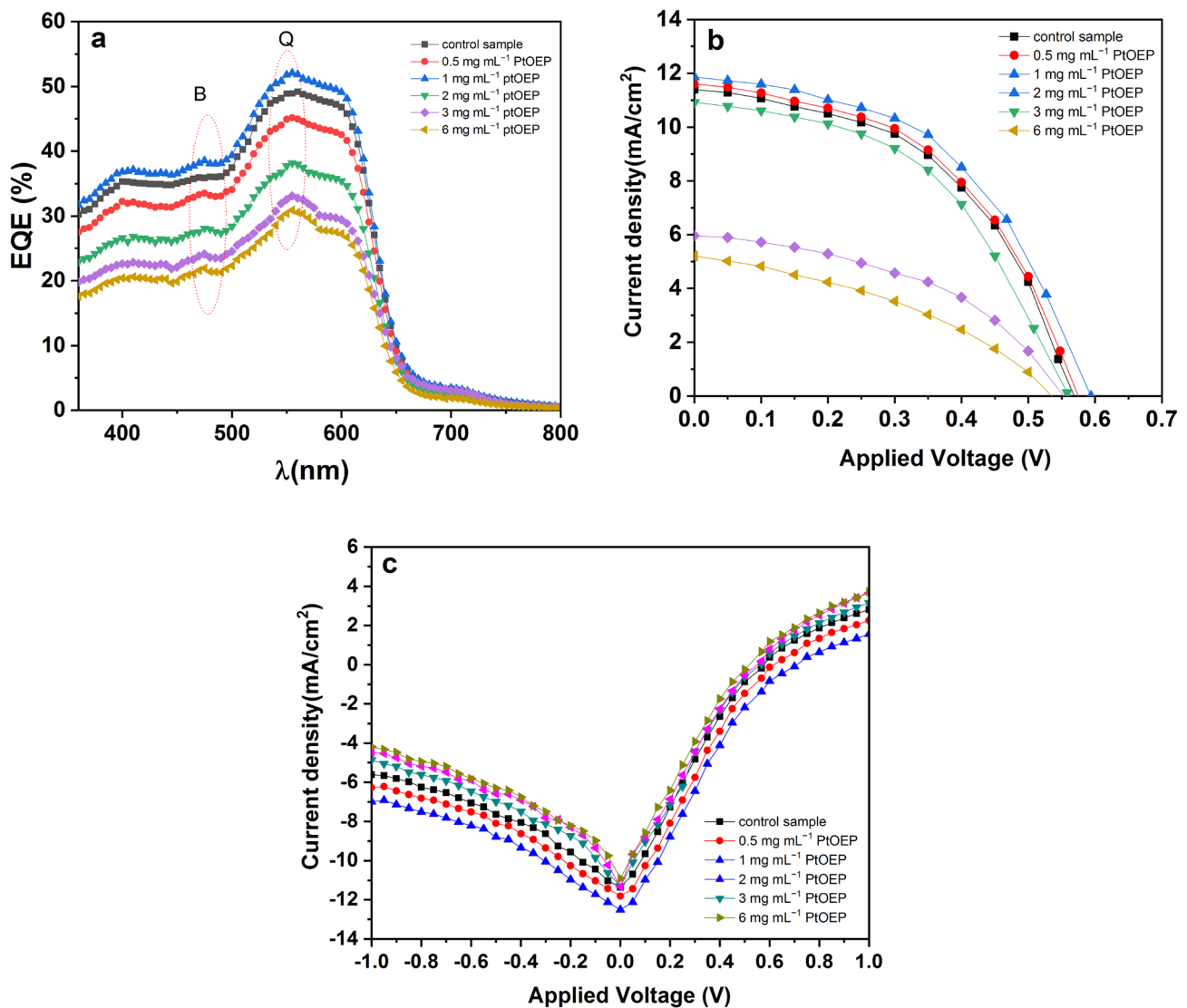
Fig. 4 **a** EQE for the solar cell solar cells based on P3HT:PCBM:PtOEP (0–6 mg mL^{-1}), **b** I–V characteristics for the solar cell with increasing the volume of PtOEP devices and **c** dark I–V characteristics of devices

Table 1 Photovoltaic of PSCs based on P3HT:PCBM:PtOEP (0, 0.5, 1, 2, 3, 6 mg mL^{-1})

Concentration of PtOEP	V_{OC} (Volt)	J_{SC} (mAcm^{-2})	FF	η%
Control sample	0.56 ± 0.009	11.39 ± 0.08	0.48 ± 0.005	3.06 ± 0.04
0.5 mg mL^{-1} PtOEP	0.57 ± 0.01	11.69 ± 0.09	0.49 ± 0.004	3.26 ± 0.05
1 mg mL^{-1} PtOEP	0.59 ± 0.01	11.95 ± 0.09	0.51 ± 0.004	3.61 ± 0.04
2 mg mL^{-1} PtOEP	0.55 ± 0.01	10.92 ± 0.08	0.49 ± 0.002	2.94 ± 0.02
3 mg mL^{-1} PtOEP	0.54 ± 0.01	5.96 ± 0.09	0.47 ± 0.004	1.51 ± 0.05
6 mg mL^{-1} PtOEP	0.53 ± 0.01	5.2 ± 0.09	0.38 ± 0.004	1.05 ± 0.07

peaks for P3HT:PCBM:PtOEP (1 mg) contribute significantly to the formation of a charge-transfer complex (CTC) in the blended films [9]. At concentration (1 mg mL^{-1}) of PtOEP, the polymer degree increase is sensitive to Raman shift C=C [1453 cm^{-1}] stretching to lower wavenumbers [1445 cm^{-1}] (see Fig. 2b) [9, 16]. However, this interaction was diminished at higher PtOEP doping concentrations (6 mg) owing to PtOEP aggregation. However, this
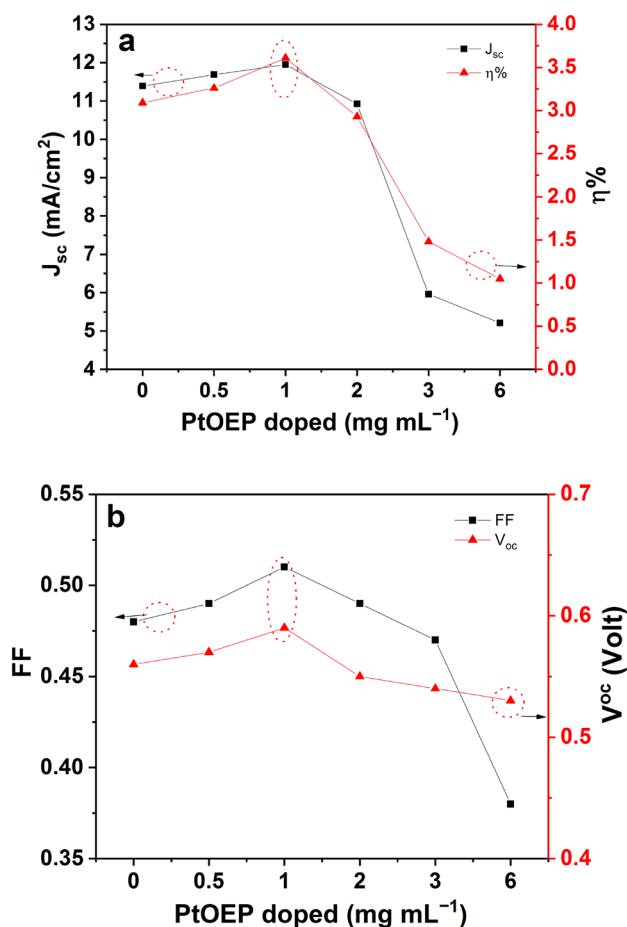
Fig. 5 Variation of **a** J_{SC} and η% and **b** FF and V_{OC} of the solar cells with increasing the volume of PtOEP

interaction is diminished at higher PtOEP doping concentrations (6 mg mL^{-1}) owing to PtOEP aggregation, and SEM images Fig. 3a–c demonstrate the existence of these aggregates. The surface of the active layer's surface seems to be smooth and homogenous at concentrations (0, 0.5, and 1 mg mL^{-1}) of PtOEP. As the doping percentage increases, PtOEP particles agglomerate on specimen surfaces with varying shapes and sizes. As a result of these aggregates defining isolated zones, charging carriers in such areas would be unable to engage in electrical transport activities effectively.

Figure 4a illustrates the external quantum efficiency (EQE) spectra of the ITO/PEDOT:PSS/P3HT:PCBM:PtOEP (0, 1 and 6 mg mL^{-1})/Al solar cells are shown in the absorption region for P3HT:PCBM:PtOEP (360–800) nm. Furthermore, at PtOEP (1 mg mL^{-1}), the maximum EQE at 550 nm increases from 49.6 to 56.8%. The effect of PtOEP doping on the efficiency of P3HT:PCBM (1:1) PSCs is seen in Fig. 4b. Table 1 displays the average photovoltaic characteristics for this system P3HT:PCBM:PtOEP (0, 0, 5, 1, 2, 3, and 6 mg mL^{-1}), including open-circuit voltage

(V_{OC}), short-circuit current density (J_{SC}), fill factor (FF), and power conversion efficiency (PCE, η%). The obtained results indicate that the V_{OC}, J_{SC} and FF are remarkably improved after adding low concentration of PtOEP. When the dopant concentration is 1 mg mL^{-1}, the J–V curves record the ideal cell parameters, which is compatible with the EQE spectra at the same concentration. In comparison to the reference cell, which had a PCE of 3.06%, the maximum PCE of 3.61% implies a 16.82% improvement. The comparative statistical parameters (including the mean values and standard deviations of JSC and PCE) are also listed in Table 1. However, when the PtOEP ratios are increased (2, 3, and 6 mg mL^{-1}), the photovoltaic performance of the samples decreases, as demonstrated in Table 1 and Fig. 5a, b. The rise in the J_{SC} may be related to an improvement in charge-carrier transfer, which is facilitated by the increasing conjugation length in the P3HT:PCBM blends owing to the PtOEP concentration in the blends. Furthermore, the lower percentage of PtOEP may change excitons from singlet into triplet excitons, resulting in higher exciton diffusion time and solar cell performance [9, 11–13, 17]. The improved performance of P3HT:PCBM:PtOEP devices might be attributed to improved morphology for electron and hole transport along the PCBM and P3HT phases. However, at higher PtOEP doping levels, the large quantities of PtOEP form big aggregates within the P3HT:PCBM, decreasing the film adhesion to the ITO substrate. The triplet excitons will be placed or restricted in these isolated areas in the PtOEP aggregation (isolated areas) even though they do not have any effective function. Moreover, these aggregations have a negative impact on solar cell efficiency, resulting in poorer JSC and PCE. The smaller FF also indicates that electron and hole carrier concentrations in systems with high concentrations are lopsided [9, 18]. Under dark conditions, the J–V characteristics of the ITO/PEDOT:PSS/P3HT:PCBM:PtOEP (0, 0, 5, 1, 2, 3, 6 mg mL^{-1})/Al solar cells are shown in Fig. 4c. When compared to the other additional devices, ITO/PEDOT, PSS/P3HT:PCBM:PtOEP (1 mg mL^{-1})/Al had the lowest reverse dark current. This indicates that introducing PtOEP (1 mg mL^{-1}) into the active layer may marginally diminish the device's microscopic leak circuit and surface recombination centers [19]. Impedance spectroscopy is used to validate the photovoltaic properties of P3HT:PCBM:PtOEP (0, 5, 1, 2, 3, 6 mg mL^{-1}). Each Nyquist plot has one semicircle, which designates that there is only one type of interface process [20]. In addition, the equivalent circuit is seen in the inset of Fig. 6a. The Nyquist plot for solar cells fits into a simple circuit, as shown in the inset of Fig. 6a, with the recombination resistance (R_{rec}) and series resistance (R_s) attributed to ITO and wire contributions [20]. The fitting parameters are reported in Table 2. Furthermore, the width of the Nyquist plot is substantially influenced by the PtOEP concentration. This observation is
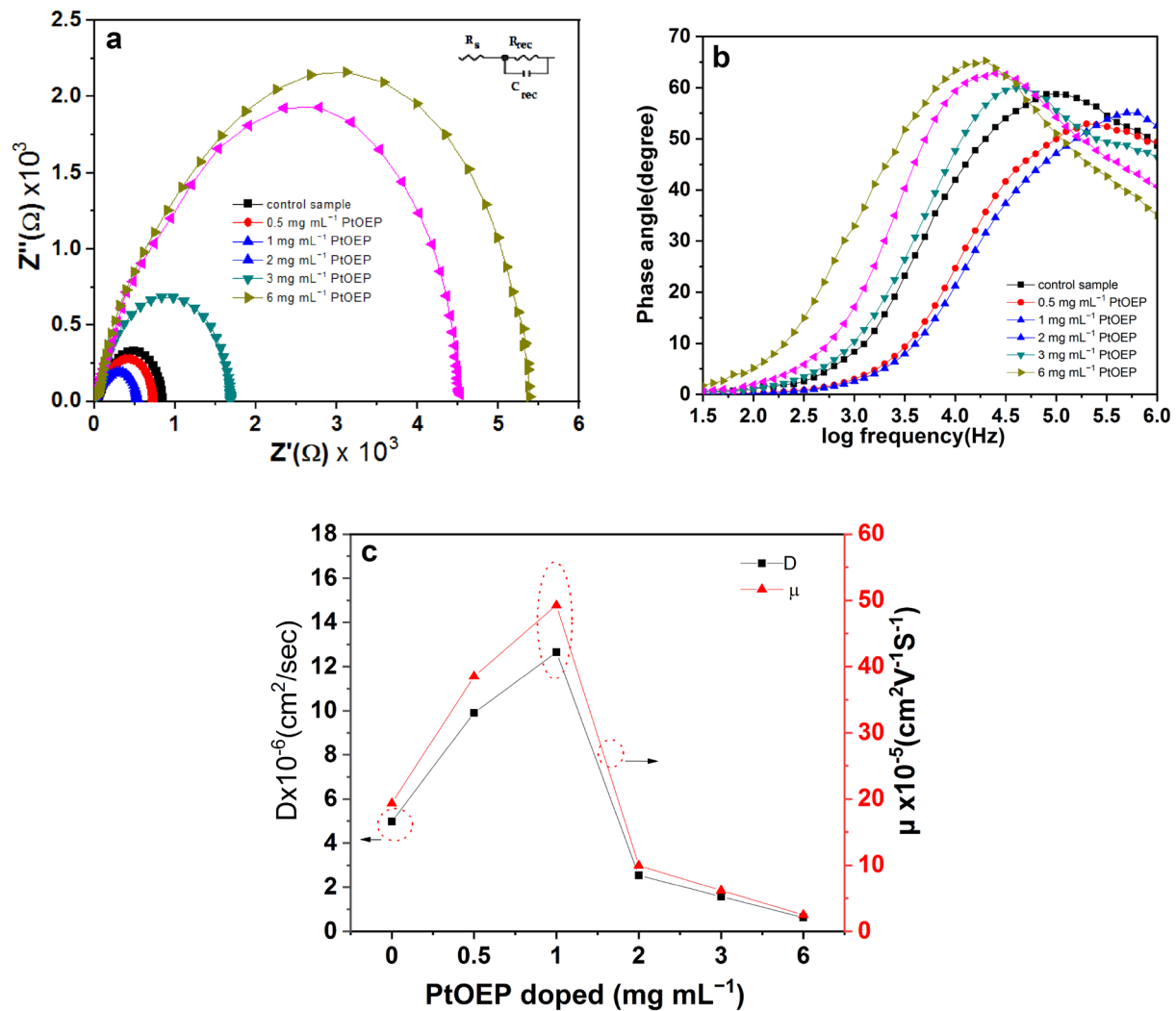
Fig. 6 **a** Impedance spectroscopy plot, and **b** Bode phase and **c** variation of D and μ of the solar cells with increasing the volume of PtOEP

Table 2 Impedance spectroscopy parameters of PSCs based on P3HT:PCBM:PtOEP (0, 0.5, 1, 2, 3, 6 mg mL^{-1})

Concentration of PtOEP	R_S (Ω)	R_{rec} (Ω)	$\tau_d \times 10^{-5}$ (S^{-1})	$D \times 10^{-6}$ ($cm^2\ S^{-1}$)	$\mu \times 10^{-5}$ ($cm^2\ V^{-1}\ S^{-1}$)
Control sample	26.6	807.4	2.01	4.97	19.35
0.5 mg mL^{-1} PtOEP	25.3	695.5	1.01	9.91	38.52
1 mg mL^{-1} PtOEP	21	503.8	0.79	12.65	49.25
2 mg mL^{-1} PtOEP	27.3	1654	3.91	2.55	9.95
3 mg mL^{-1} PtOEP	29.1	4497	6.36	1.57	6.18
6 mg mL^{-1} PtOEP	33.1	535	15.92	0.63	2.49

in accordance with the literature by Hadi et al. [20], Oklobia et al. [21], and Zhang et al. [22]. The bode phase plot (in Fig. 6b) is very valuable for estimation of the diffusion time (τ_d) of carriers through the active layer, which in turn can be used to compute the diffusion coefficient (D) and charge-carrier mobility (μ) [9, 10] (see Table 1). The lowest

values for (R_s, R_{rec}, and d) and the highest values for D and are observed when 1 mg mL^{-1} of PtOEP is introduced (see Fig. 6c). It can be assumed that the interface between P3HT and PCBM is more appropriate for charge transport in the case of using a small amount of PtOEP (0.5 and 1 mg mL^{-1}). Therefore, the electron transfer and diffusion length in the

active layer is faster and longer, resulting in higher photovoltaic properties [9, 10, 23, 24].

4 Conclusions

In summary, this study clarified the effect of PtOEP (using the blade coating method) as a phosphorescent dye with various doping levels (0.5, 1, 2, 3, and 6 mg mL^{-1}) on photovoltaic efficiency and spectroscopic impedance. We found that P3HT:PCBM devices improved their PCE by 16.82% at P3HT:PCBM:PtOEP (1 mg mL^{-1}) and had the lowest (R_s, R_{rec}, and d) and highest (D and) values. The IS results indicated that the maximum mobility value and diffusion coefficient were correlated to the maximum photovoltaic properties. Thus, the use of tiny concentrations of PtOEP in P3HT:PCBM blends will be a new strategy to enhance the performance of PSCs.

Declarations

References

1. C. Lee, S. Lee, G.-U. Kim, W. Lee, B.J. Kim, Chem. Rev. **119**, 8028 (2019)
2. W. Lee, H.D. Lee, J.H. Bae, J.W. Jung, Org. Elect. **39**, 85 (2016)
3. Y. Choia, G. Kima, H. Kima, S.H. Lee, S. Kwon, J. Kima, K. Lee, Nano Energy **30**, 200 (2016)
4. L. Lu, T. Zheng, Q. Wu, A.M. Schneider, D. Zhao, L. Yu, Chem. Rev. **115**, 12666 (2015)
5. W. Aloui, T. Adhikari, J.-M. Nunzi, A. Bouazizi, K. Khirouni, Mater. Sci. Semicond. Process. **39**, 575 (2015)
6. M. Gao, Z. Wang, Mater. Lett. **164**, 325 (2016)
7. Z. Liu, E.-C. Lee, Org. Electron. **24**, 101 (2015)
8. Y.A.M. Ismail, N. Kishi, T. Soga, Thin Solid Films **616**, 73 (2016)
9. A.A. Abuelwafa, M. Dongol, M.M. El-Nahass, T. Soga, J. Mol. Struct. **1202**, 127303 (2020)
10. A.A. Abuelwafa, M. Dongol, M.M. El-Nahass, T. Soga, Appl. Phys. A **124**, 266 (2018)
11. A.A. Abuelwafa, M.S.H. Choudhury, M. Dongol, M.M. El-Nahass, T. Soga, J. Mater Sci: Mater Electron. **29**, 4232 (2018)
12. C. Lee, I. Hwang, C.C. Byeon, B.H. Kim, N.C. Greenham, Adv. Funct. Mater. **20**, 2945 (2010)
13. K. Xiong, L. Hou, P. Wang, Y. Xia, D. Chen, B. Xiao, J. Lumine. **151**, 193 (2014)
14. A.A. Abuelwafa, A. El-Denglawey, M. Dongol, M.M. El-Nahass, T. Soga, J. Alloy. Compd **655**, 415 (2016)
15. A.A. Abuelwafa, A. El-Denglawey, M. Dongol, M.M. El-Nahass, T. Soga, Opt. Mater. **49**, 271 (2015)
16. T.-C. Wang, Y.-H. Su, Y.-K. Hung, C.-S. Yeh, L.-W. Huang, W. Gomulya, L.-H. Lai, M.A. Loi, J.-S. Yanga, J.-J. Wu, Phys. Chem. Chem. Phys. **17**, 19854 (2015)
17. F.A. Angel, C.W. Tang, Org. Electron. **30**, 247 (2016)
18. X. Gong, Y. Jiang, C. Zhang, L. Yang, M. Li, H. Ma, Appl. Phys. A **122**, 287 (2016)
19. C.-E. Cheng, Z. Pei, C.-C. Hsu, C.-S. Chang, F.S.-S. Chien, Sol. Energy Mater. Sol. Cells **121**, 80 (2014)
20. A.A. Abuelwafa, A. El-Denglawey, M. Dongol, M.M. El-Nahass, M.S. Ebied, T. Soga, Appl. Phys. A **124**, 33 (2018)
21. A. Hadi, M.H. Hekmatshoar, F. Abbasi, S. Agbolaghi, Carbon Lett. **31**, 107 (2021)
22. O. Oklobia, S. Komilian, T.S. Shafai, Organ. Electron. **61**, 276 (2018)
23. Y. Zhang, L. Li, S. Yuan, G. Li, W. Zhang, Electrochim. Acta **109**, 221 (2013)
24. W. Aloui, T. Adhikari, J.-M. Nunzi, A. Bouazizi, Mater. Res. Bull. **78**, 141 (2016)